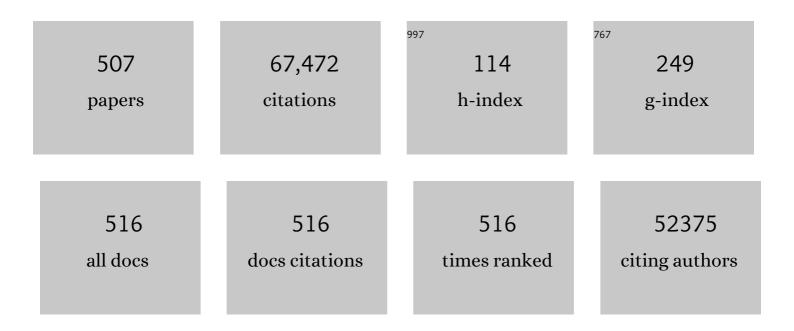
Alex K Zettl

List of Publications by Year in descending order

Source: https://exaly.com/author-pdf/636455/publications.pdf Version: 2024-02-01



Δι εν Κ Ζεττι

#	Article	IF	CITATIONS
1	Direct observation of a widely tunable bandgap in bilayer graphene. Nature, 2009, 459, 820-823.	27.8	3,148
2	Extreme Oxygen Sensitivity of Electronic Properties of Carbon Nanotubes. Science, 2000, 287, 1801-1804.	12.6	2,777
3	Graphene plasmonics for tunable terahertz metamaterials. Nature Nanotechnology, 2011, 6, 630-634.	31.5	2,566
4	High-performance transition metal–doped Pt ₃ Ni octahedra for oxygen reduction reaction. Science, 2015, 348, 1230-1234.	12.6	1,623
5	Gate-Variable Optical Transitions in Graphene. Science, 2008, 320, 206-209.	12.6	1,433
6	Strain-Induced Pseudo–Magnetic Fields Greater Than 300 Tesla in Graphene Nanobubbles. Science, 2010, 329, 544-547.	12.6	1,367
7	Single-Electron Transport in Ropes of Carbon Nanotubes. Science, 1997, 275, 1922-1925.	12.6	1,278
8	Low-Friction Nanoscale Linear Bearing Realized from Multiwall Carbon Nanotubes. Science, 2000, 289, 602-604.	12.6	1,206
9	Graphene at the Edge: Stability and Dynamics. Science, 2009, 323, 1705-1708.	12.6	1,153
10	Crossed Nanotube Junctions. Science, 2000, 288, 494-497.	12.6	1,135
11	Rotational actuators based on carbon nanotubes. Nature, 2003, 424, 408-410.	27.8	1,098
12	Direct Imaging of Lattice Atoms and Topological Defects in Graphene Membranes. Nano Letters, 2008, 8, 3582-3586.	9.1	1,090
13	Determination of the Local Chemical Structure of Graphene Oxide and Reduced Graphene Oxide. Advanced Materials, 2010, 22, 4467-4472.	21.0	1,044
14	Solid-State Thermal Rectifier. Science, 2006, 314, 1121-1124.	12.6	1,043
15	High-Resolution EM of Colloidal Nanocrystal Growth Using Graphene Liquid Cells. Science, 2012, 336, 61-64.	12.6	989
16	Tunable Phonon Polaritons in Atomically Thin van der Waals Crystals of Boron Nitride. Science, 2014, 343, 1125-1129.	12.6	957
17	Direct mechanical measurement of the tensile strength and elastic modulus of multiwalled carbon nanotubes. Materials Science & Engineering A: Structural Materials: Properties, Microstructure and Processing, 2002, 334, 173-178.	5.6	951
18	An atomic-resolution nanomechanical mass sensor. Nature Nanotechnology, 2008, 3, 533-537.	31.5	944

#	Article	IF	CITATIONS
19	The two-dimensional phase of boron nitride: Few-atomic-layer sheets and suspended membranes. Applied Physics Letters, 2008, 92, .	3.3	895
20	Nanotube Nanodevice. Science, 1997, 278, 100-102.	12.6	869
21	Observation of moiré excitons in WSe2/WS2 heterostructure superlattices. Nature, 2019, 567, 76-80.	27.8	791
22	Origin of spatial charge inhomogeneity in graphene. Nature Physics, 2009, 5, 722-726.	16.7	630
23	Spatially resolving edge states of chiral grapheneÂnanoribbons. Nature Physics, 2011, 7, 616-620.	16.7	628
24	Graphene as a Long-Term Metal Oxidation Barrier: Worse Than Nothing. ACS Nano, 2013, 7, 5763-5768.	14.6	600
25	Ultralow contact resistance between semimetal and monolayer semiconductors. Nature, 2021, 593, 211-217.	27.8	579
26	Grain Boundary Mapping in Polycrystalline Graphene. ACS Nano, 2011, 5, 2142-2146.	14.6	566
27	Local Electronic Properties of Graphene on a BN Substrate via Scanning Tunneling Microscopy. Nano Letters, 2011, 11, 2291-2295.	9.1	539
28	Characterization of collective ground states in single-layer NbSe2. Nature Physics, 2016, 12, 92-97.	16.7	536
29	Mott and generalized Wigner crystal states in WSe2/WS2 moiré superlattices. Nature, 2020, 579, 359-363.	27.8	536
30	Evolution of interlayer coupling in twisted molybdenum disulfide bilayers. Nature Communications, 2014, 5, 4966.	12.8	533
31	On the roughness of single- and bi-layer graphene membranes. Solid State Communications, 2007, 143, 101-109.	1.9	530
32	Boron Nitride Nanotubes Are Noncytotoxic and Can Be Functionalized for Interaction with Proteins and Cells. Journal of the American Chemical Society, 2009, 131, 890-891.	13.7	522
33	Topological valley transport at bilayer graphene domain walls. Nature, 2015, 520, 650-655.	27.8	502
34	Controlling inelastic light scattering quantum pathways in graphene. Nature, 2011, 471, 617-620.	27.8	492
35	Raman Spectroscopy Study of Rotated Double-Layer Graphene: Misorientation-Angle Dependence of Electronic Structure. Physical Review Letters, 2012, 108, 246103.	7.8	486
36	Imaging and dynamics of light atoms and molecules on graphene. Nature, 2008, 454, 319-322.	27.8	475

#	Article	IF	CITATIONS
37	Fully collapsed carbon nanotubes. Nature, 1995, 377, 135-138.	27.8	466
38	Atomically thin hexagonal boron nitride probed by ultrahigh-resolution transmission electron microscopy. Physical Review B, 2009, 80, .	3.2	456
39	Drude conductivity of Dirac fermions in graphene. Physical Review B, 2011, 83, .	3.2	447
40	Breakdown of Fourier's Law in Nanotube Thermal Conductors. Physical Review Letters, 2008, 101, 075903.	7.8	425
41	Synthesis ofBxCyNznanotubules. Physical Review B, 1995, 51, 11229-11232.	3.2	413
42	Giant phonon-induced conductance in scanning tunnelling spectroscopy of gate-tunable graphene. Nature Physics, 2008, 4, 627-630.	16.7	404
43	Charge density wave conduction: A novel collective transport phenomenon in solids. Physics Reports, 1985, 119, 117-232.	25.6	393
44	A cell nanoinjector based on carbon nanotubes. Proceedings of the National Academy of Sciences of the United States of America, 2007, 104, 8218-8222.	7.1	366
45	Nanotube Radio. Nano Letters, 2007, 7, 3508-3511.	9.1	366
46	High Surface Area MoS ₂ /Graphene Hybrid Aerogel for Ultrasensitive NO ₂ Detection. Advanced Functional Materials, 2016, 26, 5158-5165.	14.9	357
47	lsotope Effect on the Thermal Conductivity of Boron Nitride Nanotubes. Physical Review Letters, 2006, 97, 085901.	7.8	349
48	Fermi velocity engineering in graphene by substrate modification. Scientific Reports, 2012, 2, .	3.3	344
49	Boron nitride substrates for high mobility chemical vapor deposited graphene. Applied Physics Letters, 2011, 98, .	3.3	339
50	A direct transfer of layer-area graphene. Applied Physics Letters, 2010, 96, .	3.3	335
51	Coating Single-Walled Carbon Nanotubes with Tin Oxide. Nano Letters, 2003, 3, 681-683.	9.1	325
52	Ultrahigh Frequency Nanotube Resonators. Physical Review Letters, 2006, 97, 087203.	7.8	298
53	Search for Isotope Effect in Superconducting Y-Ba-Cu-O. Physical Review Letters, 1987, 58, 2337-2339.	7.8	293
54	Packing C60 in Boron Nitride Nanotubes. Science, 2003, 300, 467-469.	12.6	292

Alex K Zettl

#	Article	IF	CITATIONS
55	Carbon nanotubes as nanoscale mass conveyors. Nature, 2004, 428, 924-927.	27.8	291
56	Interfacing Carbon Nanotubes with Living Cells. Journal of the American Chemical Society, 2006, 128, 6292-6293.	13.7	290
57	Photoinduced doping in heterostructures of graphene and boron nitride. Nature Nanotechnology, 2014, 9, 348-352.	31.5	287
58	Multiply folded graphene. Physical Review B, 2011, 83, .	3.2	269
59	Electrical Control of Optical Plasmon Resonance with Graphene. Nano Letters, 2012, 12, 5598-5602.	9.1	266
60	Hydrocarbon lithography on graphene membranes. Applied Physics Letters, 2008, 92, .	3.3	252
61	Measurement of the intrinsic strength of crystalline and polycrystalline graphene. Nature Communications, 2013, 4, .	12.8	246
62	3D structure of individual nanocrystals in solution by electron microscopy. Science, 2015, 349, 290-295.	12.6	238
63	Gate-controlled ionization and screening of cobalt adatoms on a graphene surface. Nature Physics, 2011, 7, 43-47.	16.7	233
64	Interlayer Forces and Ultralow Sliding Friction in Multiwalled Carbon Nanotubes. Physical Review Letters, 2006, 97, 025501.	7.8	231
65	Electronic and plasmonic phenomena at graphene grain boundaries. Nature Nanotechnology, 2013, 8, 821-825.	31.5	226
66	Atomic Resolution Imaging of Grain Boundary Defects in Monolayer Chemical Vapor Deposition-Grown Hexagonal Boron Nitride. Journal of the American Chemical Society, 2013, 135, 6758-6761.	13.7	225
67	Observing Atomic Collapse Resonances in Artificial Nuclei on Graphene. Science, 2013, 340, 734-737.	12.6	223
68	ls the Intrinsic Thermoelectric Power of Carbon Nanotubes Positive?. Physical Review Letters, 2000, 85, 4361-4364.	7.8	222
69	Identifying carbon as the source of visible single-photon emission from hexagonal boron nitride. Nature Materials, 2021, 20, 321-328.	27.5	210
70	Single-particle mapping of nonequilibrium nanocrystal transformations. Science, 2016, 354, 874-877.	12.6	204
71	Ripping Graphene: Preferred Directions. Nano Letters, 2012, 12, 293-297.	9.1	200
72	Raman Spectroscopy and Time-Resolved Photoluminescence of BN and BxCyNzNanotubes. Nano Letters, 2004, 4, 647-650.	9.1	194

#	Article	IF	CITATIONS
73	Near-Edge X-Ray Absorption Fine-Structure Investigation of Graphene. Physical Review Letters, 2008, 101, 066806.	7.8	194
74	Enhanced Solid-State Order and Field-Effect Hole Mobility through Control of Nanoscale Polymer Aggregation. Journal of the American Chemical Society, 2013, 135, 19229-19236.	13.7	194
75	Characterization and manipulation of individual defects in insulating hexagonal boron nitride using scanning tunnelling microscopy. Nature Nanotechnology, 2015, 10, 949-953.	31.5	192
76	An atlas of carbon nanotube optical transitions. Nature Nanotechnology, 2012, 7, 325-329.	31.5	186
77	3D Motion of DNA-Au Nanoconjugates in Graphene Liquid Cell Electron Microscopy. Nano Letters, 2013, 13, 4556-4561.	9.1	184
78	Giant out-of-plane magnetoresistance in Bi-Sr-Ca-Cu-O: A new dissipation mechanism in copper-oxide superconductors?. Physical Review Letters, 1991, 66, 2164-2167.	7.8	179
79	Transformation of BxCyNz nanotubes to pure BN nanotubes. Applied Physics Letters, 2002, 81, 1110-1112.	3.3	179
80	Self-Assembly of Gold Nanoparticles at the Surface of Amine- and Thiol-Functionalized Boron Nitride Nanotubes. Journal of Physical Chemistry C, 2007, 111, 12992-12999.	3.1	179
81	Imaging electrostatically confined Dirac fermions in graphene quantum dots. Nature Physics, 2016, 12, 1032-1036.	16.7	176
82	Interlayer electron–phonon coupling in WSe2/hBN heterostructures. Nature Physics, 2017, 13, 127-131.	16.7	173
83	Direct Growth of Single- and Few-Layer MoS ₂ on h-BN with Preferred Relative Rotation Angles. Nano Letters, 2015, 15, 6324-6331.	9.1	172
84	Observation of an oxygen isotope shift in the superconducting transition temperature ofLa1.85Sr0.15CuO4. Physical Review Letters, 1987, 59, 915-918.	7.8	171
85	Biocompatible Carbon Nanotubes Generated by Functionalization with Glycodendrimers. Angewandte Chemie - International Edition, 2008, 47, 5022-5025.	13.8	165
86	Peeling and sharpening multiwall nanotubes. Nature, 2000, 406, 586-586.	27.8	164
87	Biomimetic Nanowire Coatings for Next Generation Adhesive Drug Delivery Systems. Nano Letters, 2009, 9, 716-720.	9.1	164
88	Graphene decoration with metal nanoparticles: Towards easy integration for sensing applications. Nanoscale, 2012, 4, 438-440.	5.6	164
89	Observation of the Giant Stark Effect in Boron-Nitride Nanotubes. Physical Review Letters, 2005, 94, 056804.	7.8	163
90	Synthesis and Characterization of Highly Crystalline Graphene Aerogels. ACS Nano, 2014, 8, 11013-11022.	14.6	162

#	Article	IF	CITATIONS
91	Imaging of pure spin-valley diffusion current in WS ₂ -WSe ₂ heterostructures. Science, 2018, 360, 893-896.	12.6	155
92	A Facile and Patternable Method for the Surface Modification of Carbon Nanotube Forests Using Perfluoroarylazides. Journal of the American Chemical Society, 2008, 130, 4238-4239.	13.7	154
93	Surface Tension Mediated Conversion of Light to Work. Journal of the American Chemical Society, 2009, 131, 5396-5398.	13.7	152
94	Graphene Nanoribbons Obtained by Electrically Unwrapping Carbon Nanotubes. ACS Nano, 2010, 4, 1362-1366.	14.6	151
95	Shrinking a Carbon Nanotube. Nano Letters, 2006, 6, 2718-2722.	9.1	149
96	Experimentally Engineering the Edge Termination of Graphene Nanoribbons. ACS Nano, 2013, 7, 198-202.	14.6	147
97	Imaging two-dimensional generalized Wigner crystals. Nature, 2021, 597, 650-654.	27.8	147
98	A tunable phonon–exciton Fano system in bilayer graphene. Nature Nanotechnology, 2010, 5, 32-36.	31.5	146
99	Precision cutting of nanotubes with a low-energy electron beam. Applied Physics Letters, 2005, 86, 053109.	3.3	143
100	Amine-functionalized boron nitride nanotubes. Solid State Communications, 2007, 142, 643-646.	1.9	139
101	Observation of Excitons in One-Dimensional Metallic Single-Walled Carbon Nanotubes. Physical Review Letters, 2007, 99, 227401.	7.8	138
102	Phase coherence in the current-carrying charge-density-wave state: ac-dc coupling experiments in NbSe3. Physical Review B, 1984, 29, 755-767.	3.2	137
103	Controlling Graphene Ultrafast Hot Carrier Response from Metal-like to Semiconductor-like by Electrostatic Gating. Nano Letters, 2014, 14, 1578-1582.	9.1	136
104	Graphene electrostatic microphone and ultrasonic radio. Proceedings of the National Academy of Sciences of the United States of America, 2015, 112, 8942-8946.	7.1	136
105	Electron Holography of Field-Emitting Carbon Nanotubes. Physical Review Letters, 2002, 88, 056804.	7.8	135
106	Graded bandgap perovskite solar cells. Nature Materials, 2017, 16, 522-525.	27.5	135
107	Onset of charge-density-wave conduction: Switching and hysteresis in NbSe3. Physical Review B, 1982, 26, 2298-2301.	3.2	127
108	Subnanometer Vacancy Defects Introduced on Graphene by Oxygen Gas. Journal of the American Chemical Society, 2014, 136, 2232-2235.	13.7	125

#	Article	IF	CITATIONS
109	Scaled Synthesis of Boron Nitride Nanotubes, Nanoribbons, and Nanococoons Using Direct Feedstock Injection into an Extended-Pressure, Inductively-Coupled Thermal Plasma. Nano Letters, 2014, 14, 4881-4886.	9.1	125
110	Longitudinal Splitting of Boron Nitride Nanotubes for the Facile Synthesis of High Quality Boron Nitride Nanoribbons. Nano Letters, 2011, 11, 3221-3226.	9.1	122
111	The Use of Graphene and Its Derivatives for Liquid-Phase Transmission Electron Microscopy of Radiation-Sensitive Specimens. Nano Letters, 2017, 17, 414-420.	9.1	120
112	The physics of boron nitride nanotubes. Physics Today, 2010, 63, 34-38.	0.3	119
113	Probing Local Strain at MX ₂ –Metal Boundaries with Surface Plasmon-Enhanced Raman Scattering. Nano Letters, 2014, 14, 5329-5334.	9.1	118
114	Imaging moiré flat bands in three-dimensional reconstructed WSe2/WS2 superlattices. Nature Materials, 2021, 20, 945-950.	27.5	118
115	Thermal conductivity of B–C–N and BN nanotubes. Applied Physics Letters, 2005, 86, 173102.	3.3	117
116	Controlled growth of a line defect in graphene and implications for gate-tunable valley filtering. Physical Review B, 2014, 89, .	3.2	117
117	Reversible disorder-order transitions in atomic crystal nucleation. Science, 2021, 371, 498-503.	12.6	117
118	Metallization of the resistivity tensor inBi2Sr2CaCu2Oxthrough epitaxial intercalation. Physical Review Letters, 1992, 68, 530-533.	7.8	115
119	Charge-Density-Wave Transport in TaS3. Physical Review Letters, 1981, 47, 64-67.	7.8	114
120	Local spectroscopy of moiré-induced electronic structure in gate-tunable twisted bilayer graphene. Physical Review B, 2015, 92, .	3.2	114
121	Mapping Dirac quasiparticles near a single Coulomb impurity on graphene. Nature Physics, 2012, 8, 653-657.	16.7	111
122	Atomically perfect torn graphene edges and their reversible reconstruction. Nature Communications, 2013, 4, 2723.	12.8	110
123	Electrostatic graphene loudspeaker. Applied Physics Letters, 2013, 102, .	3.3	109
124	Optimizing Broadband Terahertz Modulation with Hybrid Graphene/Metasurface Structures. Nano Letters, 2015, 15, 372-377.	9.1	109
125	Scanning tunneling microscopy of the charge-density-wave structure in 1T-TaS2. Physical Review B, 1994, 49, 16899-16916.	3.2	108
126	Biomimetic Engineering of Carbon Nanotubes by Using Cell Surface Mucin Mimics. Angewandte Chemie - International Edition, 2004, 43, 6111-6116.	13.8	107

Alex K Zettl

#	Article	IF	CITATIONS
127	Observation of Carrier-Density-Dependent Many-Body Effects in Graphene via Tunneling Spectroscopy. Physical Review Letters, 2010, 104, 036805.	7.8	106
128	Thermal-conductivity anisotropy of single-crystalBi2Sr2CaCu2O8. Physical Review B, 1991, 43, 408-412.	3.2	105
129	Field emission and current-voltage properties of boron nitride nanotubes. Solid State Communications, 2004, 129, 661-664.	1.9	104
130	Pyrolysis approach to the synthesis of gallium nitride nanorods. Applied Physics Letters, 2002, 80, 303-305.	3.3	103
131	Transfer-Free Batch Fabrication of Large-Area Suspended Graphene Membranes. ACS Nano, 2010, 4, 4762-4768.	14.6	103
132	Fast response integrated MEMS microheaters for ultra low power gas detection. Sensors and Actuators A: Physical, 2015, 223, 67-75.	4.1	103
133	Experimental electronic structure ofBi2CaSr2Cu2O8+δ. Physical Review B, 1989, 39, 236-242.	3.2	102
134	Localization and Nonlinear Resistance in Telescopically Extended Nanotubes. Physical Review Letters, 2004, 93, 086801.	7.8	100
135	Nanomechanics of carbon nanotubes. Philosophical Transactions Series A, Mathematical, Physical, and Engineering Sciences, 2008, 366, 1591-1611.	3.4	100
136	Nanotube Phonon Waveguide. Physical Review Letters, 2007, 99, 045901.	7.8	99
137	Activated Boron Nitride Derived from Activated Carbon. Nano Letters, 2004, 4, 173-176.	9.1	96
138	Effects of ambient humidity and temperature on the NO2 sensing characteristics of WS2/graphene aerogel. Applied Surface Science, 2018, 450, 372-379.	6.1	96
139	Epitaxial intercalation of the Bi-Sr-Ca-Cu-O superconductor series. Physical Review B, 1991, 43, 11496-11499.	3.2	95
140	A dielectric-defined lateral heterojunction in a monolayer semiconductor. Nature Electronics, 2019, 2, 60-65.	26.0	95
141	Visualization of the flat electronic band in twisted bilayer graphene near the magic angle twist. Nature Physics, 2021, 17, 184-188.	16.7	93
142	High-throughput optical imaging and spectroscopy of individual carbon nanotubes in devices. Nature Nanotechnology, 2013, 8, 917-922.	31.5	92
143	Synthesis of Highly Crystalline sp ² -Bonded Boron Nitride Aerogels. ACS Nano, 2013, 7, 8540-8546.	14.6	92
144	Probing Nanoscale Solids at Thermal Extremes. Physical Review Letters, 2007, 99, 155901.	7.8	91

#	Article	IF	CITATIONS
145	Identification of spin, valley and moir $ ilde{A}$ © quasi-angular momentum of interlayer excitons. Nature Physics, 2019, 15, 1140-1144.	16.7	91
146	Charge density wave transport in a novel inorganic chain compound, (TaSe4)2I. Solid State Communications, 1983, 46, 497-500.	1.9	89
147	Complete absence of isotope effect in YBa2Cu3O7: Consequences for phonon-mediated superconductivity. Physical Review B, 1987, 36, 3990-3993.	3.2	89
148	Anisotropic thermoelectric power and conductivity in single-crystalYBa2Cu3Oy. Physical Review B, 1988, 37, 9734-9737.	3.2	88
149	Chemicals On Demand with Phototriggerable Microcapsules. Journal of the American Chemical Society, 2009, 131, 13586-13587.	13.7	88
150	Atomic Defects in Two Dimensional Materials. Advanced Materials, 2015, 27, 5771-5777.	21.0	88
151	Symmetry breaking and nonlinear electrodynamics in the ceramic superconductor YBa2Cu3O7. Physical Review B, 1988, 37, 9840-9843.	3.2	87
152	Local charge-density-wave structure in 1T-TaS2determined by scanning tunneling microscopy. Physical Review B, 1988, 38, 10734-10743.	3.2	87
153	Growth and morphology of 0.80eV photoemitting indium nitride nanowires. Applied Physics Letters, 2004, 85, 5670-5672.	3.3	87
154	Length control and sharpening of atomic force microscope carbon nanotube tips assisted by an electron beam. Nanotechnology, 2005, 16, 2493-2496.	2.6	86
155	Highâ€temperature stability of suspended singleâ€layer graphene. Physica Status Solidi - Rapid Research Letters, 2010, 4, 302-304.	2.4	86
156	Functionalized Boron Nitride Nanotubes with a Stannic Oxide Coating:Â A Novel Chemical Route to Full Coverage. Journal of the American Chemical Society, 2003, 125, 2062-2063.	13.7	84
157	Tunable Nanoresonators Constructed from Telescoping Nanotubes. Physical Review Letters, 2006, 96, 215503.	7.8	84
158	Platinum Nanoparticle Loading of Boron Nitride Aerogel and Its Use as a Novel Material for Lowâ€Power Catalytic Gas Sensing. Advanced Functional Materials, 2016, 26, 433-439.	14.9	82
159	Tuning charge and correlation effects for a single molecule on a graphene device. Nature Communications, 2016, 7, 13553.	12.8	82
160	In Situ Localized Growth of Ordered Metal Oxide Hollow Sphere Array on Microheater Platform for Sensitive, Ultra-Fast Gas Sensing. ACS Applied Materials & Interfaces, 2017, 9, 2634-2641.	8.0	81
161	Charge-density-wave domains in 1T-TaS2observed by satellite structure in scanning-tunneling-microscopy images. Physical Review Letters, 1991, 66, 3040-3043.	7.8	79
162	Graphene Nanopore with a Self-Integrated Optical Antenna. Nano Letters, 2014, 14, 5584-5589.	9.1	79

#	Article	IF	CITATIONS
163	Identifying Defects in Nanoscale Materials. Physical Review Letters, 2004, 93, 196803.	7.8	78
164	Encapsulation of One-Dimensional Potassium Halide Crystals within BN Nanotubes. Nano Letters, 2004, 4, 1355-1357.	9.1	78
165	Alternative stacking sequences in hexagonal boron nitride. 2D Materials, 2019, 6, 021006.	4.4	78
166	Current Oscillations and Stability of Charge-Density-Wave Motion inNbSe3. Physical Review Letters, 1982, 49, 493-496.	7.8	77
167	Nanoscale Reversible Mass Transport for Archival Memory. Nano Letters, 2009, 9, 1835-1838.	9.1	76
168	Large-scale experimental and theoretical study of graphene grain boundary structures. Physical Review B, 2015, 92, .	3.2	75
169	Graphene-templated directional growth of an inorganic nanowire. Nature Nanotechnology, 2015, 10, 423-428.	31.5	75
170	Optically Discriminating Carrier-Induced Quasiparticle Band Gap and Exciton Energy Renormalization in Monolayer <mml:math <br="" xmlns:mml="http://www.w3.org/1998/Math/MathML">display="inline"><mml:mrow><mml:msub><mml:mrow><mml:mi>MoS</mml:mi></mml:mrow><mml:mn>2Physical Review Letters, 2017, 119, 087401.</mml:mn></mml:msub></mml:mrow></mml:math>	/יml:mn> י	mmi:msub> </td
171	Nanotubes from Inorganic Materials. , 2001, , 81-112.		73
172	Synthesis of aligned BxCyNz nanotubes by a substitution-reaction route. Chemical Physics Letters, 2001, 346, 368-372.	2.6	72
173	Catalytic hydrogen sensing using microheated platinum nanoparticle-loaded graphene aerogel. Sensors and Actuators B: Chemical, 2015, 206, 399-406.	7.8	72
174	Structure of boron nitride nanotubules. Applied Physics Letters, 2001, 78, 2772-2774.	3.3	71
175	Stability and dynamics of small molecules trapped on graphene. Physical Review B, 2010, 82, .	3.2	71
176	Magnetotransport properties ofLa0.6Pb0.4MnO3â^`δandNd0.6(Sr0.7Pb0.3)0.4MnO3â^`δsingle crystals. Physical Review B, 1995, 52, 9147-9150.	3.2	70
177	Complete charge density-wave mode locking and freeze-out of fluctuations inNbSe3. Physical Review B, 1985, 32, 5536-5539.	3.2	67
178	Transport properties of the superconducting oxideLa1.85Sr0.15CuO4. Physical Review B, 1987, 35, 8800-8803.	3.2	67
179	Energy gap in the high-TcsuperconductorLa1.85Sr0.15CuO4. Physical Review B, 1987, 35, 5327-5329.	3.2	67
180	Low-power, fast, selective nanoparticle-based hydrogen sulfide gas sensor. Applied Physics Letters, 2012, 100, .	3.3	67

#	Article	IF	CITATIONS
181	GaN nanorods coated with pure BN. Applied Physics Letters, 2002, 81, 5051-5053.	3.3	65
182	Nanocrystal-Powered Nanomotor. Nano Letters, 2005, 5, 1730-1733.	9.1	65
183	Tunneling spectroscopy in Bi2Sr2CaCu2O8: Is the energy gap anisotropic?. Solid State Communications, 1989, 70, 1055-1058.	1.9	64
184	Thermodynamic characterization of fullerene (C60) by differential scanning calorimetry. The Journal of Physical Chemistry, 1992, 96, 5151-5156.	2.9	64
185	Reversible writing of high-mobility and high-carrier-density doping patterns in two-dimensional van der Waals heterostructures. Nature Electronics, 2020, 3, 99-105.	26.0	64
186	Nonlinear electrodynamics in the granular superconductor YBa2Cu3O7: Experiments and interpretation. Physical Review B, 1989, 39, 11526-11537.	3.2	63
187	Tunable Graphene dc Superconducting Quantum Interference Device. Nano Letters, 2009, 9, 198-199.	9.1	63
188	Tunable Superconducting Phase Transition in Metal-Decorated Graphene Sheets. Physical Review Letters, 2010, 104, 047001.	7.8	63
189	Van der Waals-coupled electronic states in incommensurate double-walled carbon nanotubes. Nature Physics, 2014, 10, 737-742.	16.7	63
190	Elastic properties of a van der Waals solid:C60. Physical Review B, 1992, 46, 12737-12739.	3.2	62
191	Probing the Out-of-Plane Distortion of Single Point Defects in Atomically Thin Hexagonal Boron Nitride at the Picometer Scale. Physical Review Letters, 2011, 106, 126102.	7.8	62
192	Field and frequency dependence of charge-density-wave conduction in NbSe3. Physical Review B, 1981, 24, 7247-7257.	3.2	60
193	Charge-density-wave transport in orthorhombic TaS3. I. Nonlinear conductivity. Physical Review B, 1982, 26, 5760-5772.	3.2	60
194	Electron-scattering mechanisms in single-crystalK3C60. Physical Review B, 1992, 46, 12064-12067.	3.2	60
195	Nanoscale Control of Rewriteable Doping Patterns in Pristine Graphene/Boron Nitride Heterostructures. Nano Letters, 2016, 16, 1620-1625.	9.1	60
196	Molecular Arrangement and Charge Transfer in C ₆₀ /Graphene Heterostructures. ACS Nano, 2017, 11, 4686-4693.	14.6	60
197	3D MoS ₂ Aerogel for Ultrasensitive NO ₂ Detection and Its Tunable Sensing Behavior. Advanced Materials Interfaces, 2017, 4, 1700217.	3.7	60
198	Torsional instability in the single-chain limit of a transition metal trichalcogenide. Science, 2018, 361, 263-266.	12.6	60

#	Article	IF	CITATIONS
199	Observation of narrow-band charge-density-wave noise in TaS3. Physical Review B, 1981, 23, 6813-6815.	3.2	59
200	Observation of Shapiro steps in the charge-density-wave state of NbSe3. Solid State Communications, 1983, 46, 501-504.	1.9	59
201	Tunneling measurement of the energy gap in Y-Ba-Cu-O. Physical Review B, 1987, 35, 8853-8855.	3.2	59
202	Screening-Engineered Field-Effect Solar Cells. Nano Letters, 2012, 12, 4300-4304.	9.1	58
203	Charge-Carrier Screening in Single-Layer Graphene. Physical Review Letters, 2013, 110, 146802.	7.8	58
204	Nanoscale electronic devices on carbon nanotubes. Nanotechnology, 1998, 9, 153-157.	2.6	57
205	In Situ Localized Growth of Porous Tin Oxide Films on Low Power Microheater Platform for Low Temperature CO Detection. ACS Sensors, 2016, 1, 339-343.	7.8	57
206	The ultrafast onset of exciton formation in 2D semiconductors. Nature Communications, 2020, 11, 5277.	12.8	57
207	Charge-density-wave transport in orthorhombic TaS3. II. Frequency-dependent conductivity. Physical Review B, 1982, 26, 5773-5785.	3.2	56
208	Elastic response of polycrystalline and single-crystal YBa2Cu3O7. Physical Review B, 1988, 38, 11949-11951.	3.2	56
209	Crystal structure of stage-1 iodine-intercalated superconducting IBi2Sr2CaCu2Ox. Physica C: Superconductivity and Its Applications, 1991, 181, 18-24.	1.2	56
210	Sustained Mechanical Self-Oscillations in Carbon Nanotubes. Nano Letters, 2010, 10, 1728-1733.	9.1	55
211	Graphene Veils and Sandwiches. Nano Letters, 2011, 11, 3290-3294.	9.1	54
212	Quantum-coupled radial-breathing oscillations in double-walled carbon nanotubes. Nature Communications, 2013, 4, 1375.	12.8	54
213	Fabrication of Subnanometer-Precision Nanopores in Hexagonal Boron Nitride. Scientific Reports, 2017, 7, 15096.	3.3	54
214	Elasticity studies ofLa2â^'xSrxCuO4. Physical Review B, 1987, 35, 8785-8787.	3.2	53
215	c-axis stress dependence of normal and superconducting state properties ofYBa2Cu3O7. Physical Review B, 1989, 39, 4231-4234.	3.2	52
216	Soldering to a single atomic layer. Applied Physics Letters, 2007, 91, .	3.3	52

#	Article	IF	CITATIONS
217	Buckling and kinking force measurements on individual multiwalled carbon nanotubes. Physical Review B, 2007, 76, .	3.2	52
218	Subangstrom Edge Relaxations Probed by Electron Microscopy in Hexagonal Boron Nitride. Physical Review Letters, 2012, 109, 205502.	7.8	52
219	Sculpting Liquids with Two-Dimensional Materials: The Assembly of Ti ₃ C ₂ T _{<i>x</i>} MXene Sheets at Liquid–Liquid Interfaces. ACS Nano, 2019, 13, 12385-12392.	14.6	52
220	Oxygen isotope study of YBa2Cu3O7. Physical Review B, 1989, 39, 2269-2278.	3.2	51
221	Identifying different stacking sequences in few-layer CVD-grown <mml:math xmlns:mml="http://www.w3.org/1998/Math/MathML"><mml:mrow><mml:mi>Mo</mml:mi><mml:msub><mml:m mathvariant="normal">S<mml:mn>2</mml:mn></mml:m </mml:msub></mml:mrow>by low-energy atomic-resolution scanning transmission electron microscopy. Physical Review B, 2016, 93,</mml:math 	i 3.2	51
222	Thermal conductivity of single-crystal Bi-Sr-Ca-Cu-O. Physical Review B, 1990, 41, 10978-10982.	3.2	50
223	Imaging the life story of nanotube devices. Applied Physics Letters, 2005, 87, 083103.	3.3	50
224	Linear Temperature Dependent Resistivity at Constant Volume inRb3C60. Physical Review Letters, 1994, 72, 4121-4124.	7.8	49
225	Nonlinear transport and localization in single-walled carbon nanotubes. Synthetic Metals, 1999, 103, 2529-2532.	3.9	49
226	Formation and Dynamics of Electron-Irradiation-Induced Defects in Hexagonal Boron Nitride at Elevated Temperatures. Nano Letters, 2016, 16, 7142-7147.	9.1	49
227	Nonexponential relaxation in solid C60 via time-dependent singlet exciton annihilation. Chemical Physics Letters, 1995, 235, 552-557.	2.6	48
228	Efficient Fizeau drag from Dirac electrons in monolayer graphene. Nature, 2021, 594, 517-521.	27.8	48
229	Probing electronic density of states and magnetic interactions at the rare-earth site in ErBa2Cu3O7. Physical Review B, 1987, 36, 8899-8902.	3.2	47
230	Determination of superconducting and normal state parameters of single crystal K3C60. Solid State Communications, 1993, 86, 643-646.	1.9	47
231	Rubidium isotope effect in superconductingRb3C60. Physical Review Letters, 1994, 72, 3706-3709.	7.8	46
232	Nucleation and growth of InN thin films using conventional and pulsed MOVPE. Journal of Crystal Growth, 2004, 272, 400-406.	1.5	46
233	Performance Enhancement of a Graphene-Zinc Phosphide Solar Cell Using the Electric Field-Effect. Nano Letters, 2014, 14, 4280-4285.	9.1	45
234	Molecular Self-Assembly in a Poorly Screened Environment: F ₄ TCNQ on Graphene/BN. ACS Nano, 2015, 9, 12168-12173.	14.6	45

#	Article	IF	CITATIONS
235	Charge-density-wave dynamics in TaS3. Physical Review B, 1982, 25, 2081-2084.	3.2	44
236	Non-carbon nanotubes. Advanced Materials, 1996, 8, 443-445.	21.0	44
237	Instability of two-dimensional graphene: Breaking < mml:math xmlns:mml="http://www.w3.org/1998/Math/MathML" display="inline"> < mml:mrow> < mml:msup> < mml:mrow> < mml:mi> s < /mml:mi> < mml:mi> p < /mml:mi> < /mml:mrov with soft x rays. Physical Review B. 2009. 80	v>∛ <mark>ffiml:</mark> m	ın > 44
238	Switching and Phase-Slip Centers in Charge-Density-Wave Conductors. Physical Review Letters, 1986, 56, 2399-2402.	7.8	43
239	High-pressure electrical conductivity measurements in the copper oxides. Physical Review B, 1989, 40, 10973-10976.	3.2	43
240	Nanomechanical radio transmitter. Physica Status Solidi (B): Basic Research, 2008, 245, 2323-2325.	1.5	43
241	Electronic and optical properties of metal-nanoparticle filled graphene sandwiches. Applied Physics Letters, 2013, 102, .	3.3	43
242	Frequency-dependent charge transport in a one-dimensional disordered metal. Physical Review B, 1981, 24, 7474-7477.	3.2	42
243	Temperature-dependent far-infrared reflectance of La-Sr-Cu-O and La-Ca-Cu-O: Bardeen-Cooper-Schrieffer electrodynamics but uncertain energy gap. Physical Review B, 1988, 37, 1587-1593.	3.2	42
244	Kevlar Functionalized Carbon Nanotubes for Next-Generation Composites. Chemistry of Materials, 2010, 22, 2164-2171.	6.7	42
245	Simplified synthesis of double-wall carbon nanotubes. Solid State Communications, 2003, 126, 359-362.	1.9	41
246	Surface-tension-driven nanoelectromechanical relaxation oscillator. Applied Physics Letters, 2005, 86, 123119.	3.3	41
247	Thermal conductivity of B-C-N and BN nanotubes. Journal of Vacuum Science & Technology an Official Journal of the American Vacuum Society B, Microelectronics Processing and Phenomena, 2005, 23, 1883.	1.6	41
248	Nanoscale structure and superhydrophobicity of sp ² -bonded boron nitride aerogels. Nanoscale, 2015, 7, 10449-10458.	5.6	41
249	Visualization and Control of Single-Electron Charging in Bilayer Graphene Quantum Dots. Nano Letters, 2018, 18, 5104-5110.	9.1	41
250	Boron Doping and Defect Engineering of Graphene Aerogels for Ultrasensitive NO ₂ Detection. Journal of Physical Chemistry C, 2018, 122, 20358-20365.	3.1	41
251	Ultrahigh-Temperature Ceramic Aerogels. Chemistry of Materials, 2019, 31, 3700-3704.	6.7	41
252	Conserved Atomic Bonding Sequences and Strain Organization of Graphene Grain Boundaries. Nano Letters, 2014, 14, 7057-7063.	9.1	40

#	Article	IF	CITATIONS
253	Charge density wave transition and nonlinear conductivity in NbS3. Solid State Communications, 1982, 43, 345-347.	1.9	39
254	Chaotic response of NbSe3: Evidence for a new charge-density-wave phase. Physical Review B, 1984, 29, 7076-7078.	3.2	39
255	Role of current oscillations in ac-dc interference effects inNbSe3. Physical Review B, 1984, 30, 2279-2281.	3.2	39
256	Pyrolytically grown arrays of highly aligned BxCyNz nanotubes. Applied Physics Letters, 2001, 78, 2769-2771.	3.3	39
257	Imaging and Tuning Molecular Levels at the Surface of a Gated Graphene Device. ACS Nano, 2014, 8, 5395-5401.	14.6	39
258	Surface-normal electro-optic spatial light modulator using graphene integrated on a high-contrast grating resonator. Optics Express, 2016, 24, 26035.	3.4	39
259	Global Control of Stacking-Order Phase Transition by Doping and Electric Field in Few-Layer Graphene. Nano Letters, 2020, 20, 3106-3112.	9.1	39
260	Controlled placement of highly aligned carbon nanotubes for the manufacture of arrays of nanoscale torsional actuators. Nanotechnology, 2006, 17, 434-438.	2.6	38
261	Real-Time Observation of Water-Soluble Mineral Precipitation in Aqueous Solution by In Situ High-Resolution Electron Microscopy. ACS Nano, 2016, 10, 88-92.	14.6	38
262	Broad band noise associated with the current carrying charge density wave state in TaS3. Solid State Communications, 1983, 46, 29-32.	1.9	37
263	Intercalation of Hexagonal Boron Nitride by Strong Oxidizers and Evidence for the Metallic Nature of the Products. Journal of Solid State Chemistry, 1999, 147, 74-81.	2.9	36
264	Conductometric gas sensing behavior of WS2 aerogel. FlatChem, 2017, 5, 1-8.	5.6	36
265	Blue-light-emitting color centers in high-quality hexagonal boron nitride. Physical Review B, 2019, 100,	3.2	36
266	Tunable Anion-Selective Transport through Monolayer Graphene and Hexagonal Boron Nitride. ACS Nano, 2020, 14, 2729-2738.	14.6	36
267	Imaging local discharge cascades for correlated electrons in WS2/WSe2 moiré superlattices. Nature Physics, 2021, 17, 1114-1119.	16.7	36
268	Elastic anomalies in the charge density wave conductor K0.3MoO3. Solid State Communications, 1986, 60, 789-792.	1.9	35
269	Simultaneous Sheet Cross-Linking and Deoxygenation in the Graphene Oxide Sol–Gel Transition. Journal of Physical Chemistry C, 2014, 118, 28855-28860.	3.1	35
270	Elastic Properties of Charge-Density-Wave Conductors: ac-dc Electric Field Coupling. Physical Review Letters, 1986, 56, 1952-1955.	7.8	34

#	Article	IF	CITATIONS
271	Onset of superconductivity in Y-Ba-Cu-O at 100 K. Physics Letters, Section A: General, Atomic and Solid State Physics, 1987, 120, 494-496.	2.1	34
272	Variable normal-state transport properties ofBi2Sr2CaCu2O8â^'y. Physical Review B, 1990, 41, 2526-2529.	3.2	34
273	Pulse I-V characteristics measurement to study the dissipation mechanism in epitaxial YBa2Cu3Ox thin films at high current densities. Physica C: Superconductivity and Its Applications, 1993, 206, 335-344.	1.2	34
274	Current-controlled nanotube growth and zone refinement. Applied Physics Letters, 2005, 86, 173107.	3.3	34
275	Valley-dependent exciton fine structure and Autler–Townes doublets from Berry phases in monolayer MoSe2. Nature Materials, 2019, 18, 1065-1070.	27.5	34
276	High-Performance Atomically-Thin Room-Temperature NO ₂ Sensor. Nano Letters, 2020, 20, 6120-6127.	9.1	34
277	Transport and tunneling in Bi 2 Sr 2 CaCu 2 O 8â^'x. Physica C: Superconductivity and Its Applications, 1989, 162-164, 1397-1400.	1.2	33
278	Transport through crossed nanotubes. Physica E: Low-Dimensional Systems and Nanostructures, 2000, 6, 868-871.	2.7	33
279	Molecular Dynamics and Phase Transition in One-Dimensional Crystal of C ₆₀ Encapsulated Inside Single Wall Carbon Nanotubes. ACS Nano, 2009, 3, 3878-3883.	14.6	33
280	Charge-density-wave transport in orthorhombic TaS3. III. Narrow-band "noise". Physical Review B, 1983, 28, 2091-2103.	3.2	32
281	Variable Hall coefficient inBi2Sr2CaCu2O8â^'xacross the metal-insulator transition. Physical Review B, 1989, 40, 11352-11354.	3.2	32
282	Efficient preparation of graphene liquid cell utilizing direct transfer with large-area well-stitched graphene. Chemical Physics Letters, 2016, 650, 107-112.	2.6	32
283	Negative Differential Resistance and Instability in NbSe3. Physical Review Letters, 1984, 52, 2293-2296.	7.8	31
284	Imprint of transition metaldorbitals on a graphene Dirac cone. Physical Review B, 2013, 88, .	3.2	31
285	Tuning colour centres at a twisted hexagonal boron nitride interface. Nature Materials, 2022, 21, 896-902.	27.5	31
286	High frequency conductivity in the charge density wave semiconductor TaS3. Solid State Communications, 1981, 39, 531-534.	1.9	30
287	Site-selective radiation damage of collapsed carbon nanotubes. Applied Physics Letters, 1998, 73, 2435-2437.	3.3	30
288	Tunable thermal links. Applied Physics Letters, 2007, 90, 193114.	3.3	30

#	Article	IF	CITATIONS
289	Nonlinear Luttinger liquid plasmons in semiconducting single-walled carbon nanotubes. Nature Materials, 2020, 19, 986-991.	27.5	30
290	Visualizing delocalized correlated electronic states in twisted double bilayer graphene. Nature Communications, 2021, 12, 2516.	12.8	30
291	Switching and charge-density-wave transport inNbSe3. I. dc characteristics. Physical Review B, 1988, 38, 13002-13018.	3.2	29
292	Phase slips and switching in charge-density-wave transport. Physical Review B, 1988, 38, 13047-13060.	3.2	29
293	Metastable length states of a random system:TaS3. Physical Review B, 1992, 46, 1874-1877.	3.2	29
294	Resistivity saturation in alkali-doped C60. Solid State Communications, 1995, 93, 973-977.	1.9	29
295	Investigation of the absorption edge ofC60fullerite. Physical Review B, 1995, 52, R5550-R5553.	3.2	29
296	Graphene-Sealed Flow Cells for <i>In Situ</i> Transmission Electron Microscopy of Liquid Samples. ACS Nano, 2020, 14, 9637-9643.	14.6	29
297	Elastic properties of single crystal Bi2Sr2CaCu2O8. Solid State Communications, 1989, 69, 833-836.	1.9	28
298	Pr-doping of the high-magnetoresistance perovskite. Solid State Communications, 1995, 94, 917-920.	1.9	28
299	Tuning Nanoelectromechanical Resonators with Mass Migration. Nano Letters, 2009, 9, 3209-3213.	9.1	28
300	Magnetic-Field-Induced Carrier Conversion in a Charge-Density-Wave Conductor. Physical Review Letters, 1986, 57, 619-621.	7.8	27
301	X-ray-absorption near-edge structure study oflBi2Sr2CaCu2Oy. Physical Review B, 1993, 47, 1029-1035.	3.2	27
302	High-Yield Synthesis of Boron Nitride Nanoribbons <i>via</i> Longitudinal Splitting of Boron Nitride Nanotubes by Potassium Vapor. ACS Nano, 2014, 8, 9867-9873.	14.6	27
303	The study of radiation effects in emerging micro and nano electro mechanical systems (M and NEMs). Semiconductor Science and Technology, 2017, 32, 013005.	2.0	27
304	Stabilization of NbTe ₃ , VTe ₃ , and TiTe ₃ via Nanotube Encapsulation. Journal of the American Chemical Society, 2021, 143, 4563-4568.	13.7	27
305	Dynamical response of the spin-density-wave mode in tetramethyltetraselenofulvalene hexafluorophosphate [(TMTSF)2PF6]. Physical Review B, 1982, 25, 1443-1445.	3.2	26
306	Charge density wave depinning and switching in NbSe3. Solid State Communications, 1984, 50, 813-816.	1.9	26

#	Article	IF	CITATIONS
307	Electrical-transport measurements of KC60. Physical Review B, 1995, 52, R8700-R8702.	3.2	26
308	Facets of nanotube synthesis: High-resolution transmission electron microscopy study and density functional theory calculations. Physical Review B, 2009, 79, .	3.2	26
309	C ₆₀ /Collapsed Carbon Nanotube Hybrids: A Variant of Peapods. Nano Letters, 2015, 15, 829-834.	9.1	26
310	Non-equilibrium transport in NbSe3: Effects of a temperature gradient. Solid State Communications, 1985, 53, 649-653.	1.9	25
311	Elastic properties of charge-density-wave conductors in applied electric fields. Physical Review B, 1987, 36, 2626-2637.	3.2	25
312	Temperature-dependent ac conductivity of thin percolation films. Physical Review B, 1988, 38, 10290-10296.	3.2	25
313	Enhancement of the upper critical field of MgB2 by carbon-doping. Solid State Communications, 2005, 136, 278-282.	1.9	25
314	Highâ€Field Scanning Probe Lithography in Hexadecane: Transitioning from Field Induced Oxidation to Solvent Decomposition through Surface Modification. Advanced Materials, 2007, 19, 3570-3573.	21.0	25
315	Metal-insulator transition in quasi-one-dimensional <mml:math xmlns:mml="http://www.w3.org/1998/Math/MathML"><mml:msub><mml:mi>HfTe</mml:mi><mml:mn>3in the few-chain limit. Physical Review B, 2019, 100, .</mml:mn></mml:msub></mml:math 	:m a. 2 <td>nl:1215ub></td>	nl:1215ub>
316	Plasma assisted formation of 3D highly porous nanostructured metal oxide network on microheater platform for Low power gas sensing. Sensors and Actuators B: Chemical, 2019, 301, 127067.	7.8	25
317	Spatial dependence of Raman frequencies in ordered and disordered monolayer graphene. Diamond and Related Materials, 2010, 19, 608-613.	3.9	24
318	Vacancy growth and migration dynamics in atomically thin hexagonal boron nitride under electron beam irradiation. Physica Status Solidi - Rapid Research Letters, 2011, 5, 295-297.	2.4	24
319	Selfâ€Passivation of Defects: Effects of Highâ€Energy Particle Irradiation on the Elastic Modulus of Multilayer Graphene. Advanced Materials, 2015, 27, 6841-6847.	21.0	24
320	Direct Organization of Morphology-Controllable Mesoporous SnO ₂ Using Amphiphilic Graft Copolymer for Gas-Sensing Applications. ACS Applied Materials & Interfaces, 2017, 9, 37246-37253.	8.0	24
321	Preventing Thin Film Dewetting via Graphene Capping. Advanced Materials, 2017, 29, 1701536.	21.0	23
322	Frustrated supercritical collapse in tunable charge arrays on graphene. Nature Communications, 2019, 10, 477.	12.8	23
323	Ultrahigh-resolution scanning microwave impedance microscopy of moir \tilde{A} $\mbox{\sc lattices}$ and superstructures. Science Advances, 2020, 6, .	10.3	23
324	Chaotic ac Conductivity in the Charge-Density-Wave State of(TaSe4)2I. Physical Review Letters, 1984, 53, 1387-1390.	7.8	22

#	Article	IF	CITATIONS
325	Dynamics of Symmetry-Breaking Stacking Boundaries in Bilayer MoS ₂ . Journal of Physical Chemistry C, 2017, 121, 22559-22566.	3.1	22
326	Shapiro-step spectrum and phase-velocity coherence inNbSe3in a uniform temperature gradient. Physical Review B, 1986, 33, 2883-2886.	3.2	21
327	Out-of-plane current transport in Bi2Sr2CaCu2O8 in the mixed state. Physica C: Superconductivity and Its Applications, 1993, 204, 389-393.	1.2	21
328	A new look at thermal properties of nanotubes. Physica Status Solidi (B): Basic Research, 2007, 244, 4181-4183.	1.5	21
329	Low pressure chemical vapor deposition synthesis of hexagonal boron nitride on polycrystalline metal foils. Physica Status Solidi (B): Basic Research, 2013, 250, 2727-2731.	1.5	21
330	Grapheneâ€sealed Si/SiN cavities for highâ€resolution <i>in situ</i> electron microscopy of nanoâ€confined solutions. Physica Status Solidi (B): Basic Research, 2016, 253, 2351-2354.	1.5	21
331	Correlation of Electron Tunneling and Plasmon Propagation in a Luttinger Liquid. Physical Review Letters, 2018, 121, 047702.	7.8	21
332	Noise and ac-dc interference phenomena in the charge-density-wave conductorK0.3MoO3. Physical Review B, 1989, 39, 3026-3036.	3.2	20
333	New Vortex-Matter Size Effect Observed inBi2Sr2CaCu2O8+δ. Physical Review Letters, 2001, 86, 3626-3629.	7.8	20
334	Conformational Transitions at an Sâ€Layer Growing Boundary Resolved by Cryoâ€TEM. Angewandte Chemie - International Edition, 2013, 52, 4829-4832.	13.8	20
335	Metal insulator semiconductor solar cell devices based on a Cu2O substrate utilizing h-BN as an insulating and passivating layer. Applied Physics Letters, 2015, 106, .	3.3	20
336	A Universal Wet-Chemistry Route to Metal Filling of Boron Nitride Nanotubes. Nano Letters, 2016, 16, 320-325.	9.1	20
337	Single-Photon Emitters in Boron Nitride Nanococoons. Nano Letters, 2018, 18, 2683-2688.	9.1	20
338	Switching and charge-density-wave transport inNbSe3. III. Dynamical instabilities. Physical Review B, 1988, 38, 13028-13046.	3.2	19
339	C60 intercalated graphite: Predictions and experiments. Solid State Communications, 1994, 90, 357-360.	1.9	19
340	Carbon nanostructure–aSi:H photovoltaic cells with high open-circuit voltage fabricated without dopants. Solid State Communications, 2010, 150, 561-563.	1.9	19
341	Frustration and Atomic Ordering in a Monolayer Semiconductor Alloy. Physical Review Letters, 2020, 124, 096101.	7.8	19
342	Collective-mode ac conduction in the blue bronze K0.3MoO3. Solid State Communications, 1985, 54, 683-687.	1.9	18

#	Article	IF	CITATIONS
343	Magnetothermopower of NbSe3. Solid State Communications, 1987, 61, 587-590.	1.9	18
344	Surface Atom Motion to Move Iron Nanocrystals through Constrictions in Carbon Nanotubes under the Action of an Electric Current. Physical Review Letters, 2013, 110, 185901.	7.8	18
345	Synthesis of Single‣ayer Graphene on Nickel Using a Droplet CVD Process. Advanced Materials Interfaces, 2017, 4, 1600783.	3.7	18
346	Emergence of Topologically Nontrivial Spin-Polarized States in a Segmented Linear Chain. Physical Review Letters, 2020, 124, 206403.	7.8	18
347	Revealing the BrÃ,nsted-Evans-Polanyi relation in halide-activated fast MoS ₂ growth toward millimeter-sized 2D crystals. Science Advances, 2021, 7, eabj3274.	10.3	18
348	Crystal structures of stage-n iodine-intercalated compounds IBi2nSr2nCanCu2nOx. Physica C: Superconductivity and Its Applications, 1992, 190, 597-605.	1.2	17
349	Symmetry Breaking in Boron Nitride Nanotubes. Physical Review Letters, 2006, 97, 176804.	7.8	17
350	Extreme thermal stability of carbon nanotubes. Physica Status Solidi (B): Basic Research, 2007, 244, 3960-3963.	1.5	17
351	Pacilé <i>etÂal.</i> Reply:. Physical Review Letters, 2009, 102, .	7.8	17
352	Selenium capped monolayer NbSe ₂ for twoâ€dimensional superconductivity studies. Physica Status Solidi (B): Basic Research, 2016, 253, 2396-2399.	1.5	17
353	lmaging gate-tunable Tomonaga–Luttinger liquids in 1H-MoSe2 mirror twin boundaries. Nature Materials, 2022, 21, 748-753.	27.5	17
354	ac calorimetry ofC60single crystals. Physical Review B, 1992, 45, 13831-13833.	3.2	16
355	Direct Mechanical Measurement of the Tensile Strength and Elastic Modulus of Multiwalled Carbon Nanotubes. Microscopy and Microanalysis, 2006, 12, 934-935.	0.4	16
356	Direct Fabrication of Zero- and One-Dimensional Metal Nanocrystals by Thermally Assisted Electromigration. ACS Nano, 2010, 4, 2999-3004.	14.6	16
357	Effect of gadolinium adatoms on the transport properties of graphene. Physical Review B, 2012, 86, .	3.2	16
358	Electrostatically Driven Nanoballoon Actuator. Nano Letters, 2016, 16, 6787-6791.	9.1	16
359	Low-power catalytic gas sensing using highly stable silicon carbide microheaters. Journal of Micromechanics and Microengineering, 2017, 27, 045003.	2.6	16
360	Spatially resolving density-dependent screening around a single charged atom in graphene. Physical Review B, 2017, 95, .	3.2	16

#	Article	IF	CITATIONS
361	Layer-dependent topological phase in a two-dimensional quasicrystal and approximant. Proceedings of the United States of America, 2020, 117, 26135-26140.	7.1	16
362	Nanoimaging of Low-Loss Plasmonic Waveguide Modes in a Graphene Nanoribbon. Nano Letters, 2021, 21, 3106-3111.	9.1	16
363	Ultranarrow TaS ₂ Nanoribbons. Nano Letters, 2021, 21, 3211-3217.	9.1	16
364	Complete excitation spectrum for a charge-density-wave system. Physical Review B, 1987, 36, 6708-6711.	3.2	15
365	Magnetic and resistive determination of the oxygen isotope effect in La1.85Sr0.15CuO4. Solid State Communications, 1988, 67, 707-711.	1.9	15
366	Microstructure of the highTcphase (Tcâ^¼111 K) in the Sbâ€Pbâ€Biâ€Srâ€Caâ€Cuâ€O system. Applied Physics L 58, 188-190.	etters, 19	191. 15
367	Microwave electromechanical resonator consisting of clamped carbon nanotubes in an abacus arrangement. Physical Review B, 2007, 76, .	3.2	15
368	Vibrational spectroscopy at electrolyte/electrode interfaces with graphene gratings. Nature Communications, 2015, 6, 7593.	12.8	15
369	Transient charge-density-wave dynamics inNbSe3. Physical Review B, 1985, 32, 8427-8430.	3.2	14
370	High-temperature resistivity and oxygen diffusion in Bi2Sr2CaCu2Ox. Physica C: Superconductivity and Its Applications, 1993, 209, 585-590.	1.2	14
371	Automatic software correction of residual aberrations in reconstructed HRTEM exit waves of crystalline samples. Advanced Structural and Chemical Imaging, 2016, 2, 15.	4.0	14
372	Geometry and electronic structure of iridium adsorbed on graphene. Physical Review B, 2019, 99, .	3.2	14
373	Targeting One- and Two-Dimensional Ta–Te Structures via Nanotube Encapsulation. Nano Letters, 2022, 22, 2285-2292.	9.1	14
374	On the nonlinear charge density wave conductivity of TaS3. Solid State Communications, 1981, 39, 899-901.	1.9	13
375	Frequency dependent conductivity in HfTe5 and ZrTe5. Solid State Communications, 1983, 45, 247-249.	1.9	13
376	Compositionally dependent superconducting transition temperature of Yî—,Baî—,Cu oxides. Physics Letters, Section A: General, Atomic and Solid State Physics, 1987, 123, 34-36.	2.1	13
377	Elastic properties of polycrystalline La2-xSrxCuO4. Solid State Communications, 1988, 65, 1073-1078.	1.9	13
378	The isotope and superconducting oxides. Journal of Physics C: Solid State Physics, 1988, 21, 5977-5985.	1.5	13

#	Article	IF	CITATIONS
379	Normal state a.c. conductivity of YBa2Cu3O7-Ĵ´. Solid State Communications, 1989, 70, 1059-1063.	1.9	13
380	Crystal structure of stage-2 iodine-intercalated superconducting IBi4Sr4Ca2Cu4Ox. Physica C: Superconductivity and Its Applications, 1991, 184, 127-134.	1.2	13
381	Scanning tunneling microscopy of the blue bronzes (Rb,K)0.3MoO3. Physical Review B, 1992, 45, 11474-11480.	3.2	13
382	Stabilization of the Tl2Ba2Ca2Cu3O10 superconductor by Hg doping. Physica C: Superconductivity and Its Applications, 1994, 234, 24-28.	1.2	13
383	Magnetotransport in single-crystal Rb3C60. Physica C: Superconductivity and Its Applications, 1994, 228, 175-180.	1.2	13
384	Universal Form of Hall Coefficient in K and Rb Doped Single CrystalC60. Physical Review Letters, 1995, 74, 1637-1640.	7.8	13
385	A phase-slip model of switching. Physica B: Physics of Condensed Matter & C: Atomic, Molecular and Plasma Physics, Optics, 1986, 143, 152-154.	0.9	12
386	Charge-density-wave magnetodynamics in NbSe3. Physical Review B, 1986, 34, 5970-5973.	3.2	12
387	Spontaneous twisting of a collapsed carbon nanotube. Nano Research, 2017, 10, 1942-1949.	10.4	12
388	Metalloâ€Hydrogelâ€Assisted Synthesis and Direct Writing of Transition Metal Dichalcogenides. Advanced Functional Materials, 2019, 29, 1807612.	14.9	12
389	Layer-Dependent Electronic Structure of Atomically Resolved Two-Dimensional Gallium Selenide Telluride. Nano Letters, 2019, 19, 1782-1787.	9.1	12
390	A molecular shift register made using tunable charge patterns in one-dimensional molecular arrays on graphene. Nature Electronics, 2020, 3, 598-603.	26.0	12
391	Switching and charge-density-wave transport inNbSe3. II. ac characteristics. Physical Review B, 1988, 38, 13019-13027.	3.2	11
392	Phase-contrast imaging of multiply-scattering extended objects at atomic resolution by reconstruction of the scattering matrix. Physical Review Research, 2021, 3, .	3.6	11
393	ac Dynamics of NbSe3 in the switching regime. Solid State Communications, 1985, 55, 307-310.	1.9	10
394	On the 17.5K transition in URu2Si2: thermopower and elasticity. Solid State Communications, 1987, 62, 603-607.	1.9	10
395	Pressure dependence of superconductivity in single-crystal Bi2(Sr, Ca)3Cu2O8. Solid State Communications, 1989, 70, 321-323.	1.9	10

 $_{396}$ Structural properties of stage-1 iodine-intercalated superconducting I (Bi0.915, Pb0.085)2(Sr0.93,) Tj ETQq0 0 0 rgBT /Overlock 10 Tf 5 10 T

#	Article	IF	CITATIONS
397	Transport spectroscopy of single-walled carbon nanotubes. Physica B: Condensed Matter, 1998, 249-251, 132-135.	2.7	10
398	Polymer chain orientations in KC60 and RbC60: structural analysis and relation with electronic properties. Synthetic Metals, 1999, 103, 2354-2357.	3.9	10
399	Studies of the dynamics of biological macromolecules using Au nanoparticle–DNA artificial molecules. Faraday Discussions, 2014, 175, 203-214.	3.2	10
400	Fabrication of One-Dimensional Zigzag [6,6]-Phenyl-C ₆₁ -Butyric Acid Methyl Ester Nanoribbons from Two-Dimensional Nanosheets. ACS Nano, 2015, 9, 10516-10522.	14.6	10
401	Self-Assembled PCBM Nanosheets: A Facile Route to Electronic Layer-on-Layer Heterostructures. Nano Letters, 2018, 18, 1442-1447.	9.1	10
402	Imeret al. reply. Physical Review Letters, 1989, 63, 102-102.	7.8	9
403	In-plane vortex-lattice depinning in a layered superconductor. Physical Review B, 1992, 45, 13148-13151.	3.2	9
404	Random access of nanodevices. Solid State Communications, 2000, 113, 549-552.	1.9	9
405	Probing structural phase transitions of crystalline C60 via resistivity measurements of metal film overlayers. Solid State Communications, 2003, 128, 359-363.	1.9	9
406	Nanocrystal cleaving. Applied Physics Letters, 2004, 84, 2644-2645.	3.3	9
407	Current–phase relation in graphene and application to a superconducting quantum interference device. Physica Status Solidi (B): Basic Research, 2009, 246, 2568-2571.	1.5	9
408	Communications: Nanomagnetic shielding: High-resolution NMR in carbon allotropes. Journal of Chemical Physics, 2010, 132, 021102.	3.0	9
409	Synthesis of graphene nanoribbons inside boron nitride nanotubes. Physica Status Solidi (B): Basic Research, 2016, 253, 2377-2379.	1.5	9
410	Probing subwavelength in-plane anisotropy with antenna-assisted infrared nano-spectroscopy. Nature Communications, 2021, 12, 2649.	12.8	9
411	Alkali-metal isotope effect in Rb3C60. Physica C: Superconductivity and Its Applications, 1994, 235-240, 2493-2494.	1.2	8
412	Self-assembly and metal-directed assembly of organic semiconductor aerogels and conductive carbon nanofiber aerogels with controllable nanoscale morphologies. Carbon, 2019, 153, 648-656.	10.3	8
413	Scanning tunnelling microscopy of charge density waves in 1Tâ€₹aS ₂ . Journal of Microscopy, 1988, 152, 771-778.	1.8	7
414	Far-infrared conductivity ofTaS3: The intrinsic charge-density-wave excitation modes. Physical Review B, 1991, 44, 3505-3508.	3.2	7

#	Article	IF	CITATIONS
415	Pressure dependence of the resistivity and magnetoresistance in single-crystal. Journal of Physics Condensed Matter, 1996, 8, 7723-7731.	1.8	7
416	Carbon Nanotube Electrostatic Biprism: Principle of Operation and Proof of Concept. Microscopy and Microanalysis, 2004, 10, 420-424.	0.4	7
417	A one-step process for localized surface texturing and conductivity enhancement in organic solar cells. Applied Physics Letters, 2009, 95, .	3.3	7
418	Direct measurement of the built-in potential in a nanoscale heterostructure. Physical Review B, 2010, 82, .	3.2	7
419	Polymerâ€free, low tension graphene mechanical resonators. Physica Status Solidi - Rapid Research Letters, 2013, 7, 1064-1066.	2.4	7
420	Fabrication of Gate-tunable Graphene Devices for Scanning Tunneling Microscopy Studies with Coulomb Impurities. Journal of Visualized Experiments, 2015, , e52711.	0.3	7
421	Nanopatterning Hexagonal Boron Nitride with Helium Ion Milling: Towards Atomically-Thin, Nanostructured Insulators. MRS Advances, 2018, 3, 327-331.	0.9	7
422	Electron beam-induced nanopores in Bernal-stacked hexagonal boron nitride. Applied Physics Letters, 2020, 117, .	3.3	7
423	Imaging Quantum Interference in Stadium-Shaped Monolayer and Bilayer Graphene Quantum Dots. Nano Letters, 2021, 21, 8993-8998.	9.1	7
424	Experimental and Theoretical Study of Possible Collective Electronic States in Exfoliable Re-Doped NbS ₂ . ACS Nano, 2021, 15, 18297-18304.	14.6	7
425	A novel switching phenomenon in quenched NbSe3. Solid State Communications, 1989, 70, 859-862.	1.9	6
426	Superconductivity and Chemical Composition of the High-TcPhase (Tcâ^¼111 K) in the Sb-Pb-Bi-Sr-Ca-Cu-O System. Japanese Journal of Applied Physics, 1991, 30, L99-L102.	1.5	6
427	Granularity and upper critical fields in K3C60. Physica C: Superconductivity and Its Applications, 1994, 232, 22-26.	1.2	6
428	Pressure dependence of and of a dirty two-gap superconductor, carbon-doped MgB2. Solid State Communications, 2006, 140, 163-166.	1.9	6
429	Fabrication of magnetic force microscopy probes via localized electrochemical deposition of cobalt. Journal of Vacuum Science & Technology B, 2007, 25, L39.	1.3	6
430	A Carbon Nanotube-based NEMS Parametric Amplifier for Enhanced Radio Wave Detection and Electronic Signal Amplification. Journal of Physics: Conference Series, 2011, 302, 012001.	0.4	6
431	Facile electron-beam lithography technique for irregular and fragile substrates. Applied Physics Letters, 2014, 105, 173109.	3.3	6
432	Tunable electronic structure in gallium chalcogenide van der Waals compounds. Physical Review B, 2019, 100, .	3.2	6

#	Article	IF	CITATIONS
433	Imaging Reconfigurable Molecular Concentration on a Graphene Field-Effect Transistor. Nano Letters, 2021, 21, 8770-8776.	9.1	6
434	Distinct current-carrying charge density wave states in NbSe3. Solid State Communications, 1986, 57, 27-30.	1.9	5
435	Normal-state transport properties of fullerene superconductors. Journal of Superconductivity and Novel Magnetism, 1994, 7, 639-642.	0.5	5
436	Specific heat of Mg(B1â^'xCx)2, x=0.05, 0.1. Physica C: Superconductivity and Its Applications, 2013, 485, 168-176.	1.2	5
437	Nanostructures on graphene using supramolecule and supramolecular nanocomposites. Nanoscale, 2014, 6, 4503-4507.	5.6	5
438	Microscopy of hydrogen and hydrogen-vacancy defect structures on graphene devices. Physical Review B, 2018, 98, .	3.2	5
439	Autocorrected off-axis holography of two-dimensional materials. Physical Review Research, 2020, 2, .	3.6	5
440	Kirigami Engineering of Suspended Graphene Transducers. Nano Letters, 2022, 22, 5301-5306.	9.1	5
441	A RF-induced dynamic coherence length in NbSe3. Synthetic Metals, 1987, 19, 813-818.	3.9	4
442	Stress-dependent magnetoresistance in NbSe3. Solid State Communications, 1987, 64, 417-419.	1.9	4
443	Zettl and Kinney reply. Physical Review Letters, 1988, 60, 753-753.	7.8	4
444	Domain structure and impurity length-scale effects in switching charge-density-wave conductors. Physical Review B, 1988, 37, 8817-8828.	3.2	4
445	Anomalous magnetoresistance in charge density wave compounds: Is NbSe3 unique?. Solid State Communications, 1990, 73, 477-480.	1.9	4
446	Magneto-elastic properties of NbSe3. Synthetic Metals, 1991, 43, 3863-3866.	3.9	4
447	Thermal conductivity of Bi2Sr2CaCu2O8 in the mixed state. Physica C: Superconductivity and Its Applications, 1994, 235-240, 1505-1506.	1.2	4
448	The electrodynamic response of K3C60 and Rb3C60 single crystals. Synthetic Metals, 1995, 70, 1325-1327.	3.9	4
449	Hexagonal boron nitride as a cationic diffusion barrier to form a graded band gap perovskite heterostructure. Physica Status Solidi (B): Basic Research, 2016, 253, 2478-2480.	1.5	4
450	Narrowband noise study of sliding charge density waves in NbSe ₃ nanoribbons. New Journal of Physics, 2017, 19, 023001.	2.9	4

Alex K Zettl

#	Article	IF	CITATIONS
451	Noise and Shapiro step interference in the charge-density-wave conductor K0.3MoO3. Solid State Communications, 1988, 66, 253-256.	1.9	3
452	Charge-density-wave pinning and metastable-state dynamics inNbSe3. Physical Review B, 1992, 45, 3260-3264.	3.2	3
453	Lattice-induced modulation of a charge-density wave far from commensurability. Physical Review B, 1992, 46, 9817-9820.	3.2	3
454	Phase strain model for charge density wave sub-domain formation in an applied temperature gradient. Solid State Communications, 1993, 87, 531-533.	1.9	3
455	Structural properties of vapor-grown C60 crystals. Applied Physics A: Solids and Surfaces, 1993, 57, 171-174.	1.4	3
456	Thermal properties of fullerenes. Synthetic Metals, 1993, 56, 2985-2990.	3.9	3
457	The Eliashberg electron-photon theory for the superconducting alkali-metal-doped fullerenes. Physica B: Condensed Matter, 1996, 219-220, 169-171.	2.7	3
458	Optical spectroscopy of bilayer graphene. Physica Status Solidi (B): Basic Research, 2010, 247, 2931-2934.	1.5	3
459	Excitons at the B K edge of boron nitride nanotubes probed by x-ray absorption spectroscopy. Journal of Physics Condensed Matter, 2010, 22, 295301.	1.8	3
460	Gas Sensors: Platinum Nanoparticle Loading of Boron Nitride Aerogel and Its Use as a Novel Material for Lowâ€Power Catalytic Gas Sensing (Adv. Funct. Mater. 3/2016). Advanced Functional Materials, 2016, 26, 314-314.	14.9	3
461	Coronene-Based Graphene Nanoribbons Insulated by Boron Nitride Nanotubes: Electronic Properties of the Hybrid Structure. ACS Omega, 2018, 3, 12930-12935.	3.5	3
462	One-Step Conversion of Graphite to Crinkled Boron Nitride Nanofoams for Hydrophobic Liquid Absorption. ACS Applied Nano Materials, 2021, 4, 3500-3507.	5.0	3
463	Upper limit on the resistivity of La1.85Sr0.15CuO4. Physics Letters, Section A: General, Atomic and Solid State Physics, 1987, 122, 61-63.	2.1	2
464	Pressure and magnetic field effects on transport in NbSe3. Synthetic Metals, 1991, 43, 3859-3862.	3.9	2
465	Spin-density-wave pinning in chromium. Physical Review B, 1991, 44, 5313-5315.	3.2	2
466	Effect of random noise on a mode-locked system. Physical Review B, 1991, 43, 13699-13702.	3.2	2
467	The complex permeability and harmonic generation of a Bi2Sr2CaCu2O8â^'y crystal: measurements and models. Journal of Magnetism and Magnetic Materials, 1992, 115, 197-203.	2.3	2
468	Chapter 1 Nanotubes: an experimental overview. Contemporary Concepts of Condensed Matter Science, 2008, 3, 1-27.	0.5	2

#	Article	IF	CITATIONS
469	Graphene Nanopore with Self-Aligned Plasmonic Optical Antenna. Biophysical Journal, 2014, 106, 414a.	0.5	2
470	Low power microheater-based combustible gas sensor with graphene aerogel catalyst support. , 2015, , .		2
471	High Resolution Imaging in the Graphene Liquid Cell. , 0, , 393-407.		2
472	Density Tunable Graphene Aerogels Using a Sacrificial Polycyclic Aromatic Hydrocarbon. Physica Status Solidi (B): Basic Research, 2017, 254, 1700203.	1.5	2
473	Wafer-scale on-chip synthesis and field emission properties of vertically aligned boron nitride based nanofiber arrays. Applied Physics Letters, 2019, 114, 093101.	3.3	2
474	Strain-controlled Graphene-Polymer Angular Actuator. MRS Advances, 2019, 4, 2161-2167.	0.9	2
475	Characterizing transition-metal dichalcogenide thin-films using hyperspectral imaging and machine learning. Scientific Reports, 2020, 10, 11602.	3.3	2
476	Accelerated Ultrafast Magnetization Dynamics at Graphene/CoGd Interfaces. ACS Nano, 2022, 16, 9620-9630.	14.6	2
477	Dynamics of charge density wave conductors: Broken coherence, chaos, and noisy precursors. Physica B: Physics of Condensed Matter & C: Atomic, Molecular and Plasma Physics, Optics, 1986, 143, 69-72.	0.9	1
478	Charge-density-wave switching behavior in an applied temperature gradient. Solid State Communications, 1988, 65, 791-795.	1.9	1
479	Effect of heating and rapidly quenchingNbSe3crystals. Physical Review B, 1990, 41, 1671-1672.	3.2	1
480	Construction of a low-temperature STM with in situ sample cleavage. Ultramicroscopy, 1992, 42-44, 1627-1631.	1.9	1
481	Sub-domain scaling and asymmetry in NbSe3. Solid State Communications, 1993, 87, 527-530.	1.9	1
482	Superconductivity and transport properties of Tl2â^'xHgxBa2Ca2Cu3O10â^'δ. Physica C: Superconductivity and Its Applications, 1994, 235-240, 1491-1492.	1.2	1
483	Temperature dependent resistivity in Rb3C60: constant volume versus constant pressure. Physica C: Superconductivity and Its Applications, 1994, 235-240, 2507-2508.	1.2	1
484	Bulk vortex matter inBi2Sr2CaCu2O8+δusing Corbinol disk contacts. Physical Review B, 2005, 71, .	3.2	1
485	Limits of Nanomechanical Resonators. , 2006, , .		1
486	Specific Heats of Mg(B1â^'xCx)2: Two-Gap Superconductors. AIP Conference Proceedings, 2006, , .	0.4	1

#	Article	IF	CITATIONS
487	A novel architecture for photovoltaic devices: Field-effect solar cells using screening-engineered nanoelectrodes for silicon and earth abundant cuprous oxide. , 2013, , .		1
488	Graphene-sealed Si/SiN cavities for high-resolution in situ electron microscopy of nano-confined solutions (Phys. Status Solidi B 12/2016). Physica Status Solidi (B): Basic Research, 2016, 253, 2544-2544.	1.5	1
489	Sherwin, Hall, and Zettl respond. Physical Review Letters, 1985, 55, 3008-3008.	7.8	0
490	Magnetotransport studies in charge density wave conductors. Synthetic Metals, 1987, 19, 807-812.	3.9	0
491	Temperature-gradient-induced subdomain scaling in NbSe3. Synthetic Metals, 1991, 43, 3871-3874.	3.9	0
492	Far infrared reflectance and conductivity of TaS3: Completion of the AC response spectrum. Synthetic Metals, 1991, 43, 3867-3870.	3.9	0
493	Tunable Nanoresonator. AlP Conference Proceedings, 2005, , .	0.4	0
494	A proposed measurement of controlled defect induction and annealing in a carbon nanotube. , 2008, , .		0
495	In-Situ TEM Observation of Metal Zn Nanocrystal Growth on ZnO Films. Microscopy and Microanalysis, 2009, 15, 698-699.	0.4	Ο
496	Infrared spectroscopy of graphene. , 2011, , .		0
497	Innentitelbild: Conformational Transitions at an S-Layer Growing Boundary Resolved by Cryo-TEM (Angew. Chem. 18/2013). Angewandte Chemie, 2013, 125, 4796-4796.	2.0	0
498	A novel architecture for photovoltaic devices: Field-effect solar cells using screening-engineered nanoelectrodes for silicon and earth abundant cuprous oxide. , 2013, , .		0
499	Statistical Characterization of High Angle Graphene Grain Boundaries at Atomic Resolution. Microscopy and Microanalysis, 2014, 20, 1056-1057.	0.4	0
500	In Situ High Temperature Atomic Resolution Transmission Electron Microscopy of 2D Nanomaterials. Microscopy and Microanalysis, 2014, 20, 1770-1771.	0.4	0
501	Large-Scale Molecular Dynamics and High-Resolution Transmission Electron Microscopy Study of Graphene Grain Boundaries. Microscopy and Microanalysis, 2015, 21, 1451-1452.	0.4	0
502	Identifying and Engineering the Stacking Sequence in CVD Grown Few-layer MoS2 via Aberration-corrected STEM. Microscopy and Microanalysis, 2017, 23, 2006-2007.	0.4	0
503	Graphene: Preventing Thin Film Dewetting via Graphene Capping (Adv. Mater. 36/2017). Advanced Materials, 2017, 29, .	21.0	0
504	Selective Insulation of Carbon Nanotubes. Physica Status Solidi (B): Basic Research, 2017, 254, 1700202.	1.5	0

#	Article	IF	CITATIONS
505	Electrically Driven Dynamics of Fewâ€Chain NbSe 3. Physica Status Solidi (B): Basic Research, 2019, 256, 1900241.	1.5	Ο
506	Observation of Atomic Ordering in a Monolayer Semiconductor Alloy. Microscopy and Microanalysis, 2020, 26, 2366-2367.	0.4	0
507	Response to Comment on "Reversible disorder-order transitions in atomic crystal nucleationâ€. Science, 2022, 375, eabj3683.	12.6	Ο